1-1-2011

Isochron dating of sand-loess-soil deposits from the Mu Us Desert margin, central China

Bo Li
University of Hong Kong, bli@uow.edu.au

Sheng-Hua Li
University of Hong Kong

Jimin Sun
Chinese Academy of Sciences

Isochron dating of sand-loess-soil deposits from the Mu Us Desert margin, central China

Abstract

A sand-loess-soil sequence from the margin of the Mu Us Desert was studied using the isochron infrared stimulated luminescence (IRSL) dating method utilizing K-feldspar grains extracted from sediments. Although the IRSL ages measured with the conventional method showed underestimation as a result of anomalous fading, the isochron results are broadly consistent with independent ages based on stratigraphic correlation in a glacial/interglacial scale over the last 250 ka. For samples older than 250 ka, the IRSL signals approached in field saturation and the isochron dating gave ambiguous results, suggesting an age limit for the method.

Keywords

central, margin, desert, us, mu, deposits, soil, dating, sand, china, loess, isochron, CAS

Disciplines

Medicine and Health Sciences | Social and Behavioral Sciences

Publication Details

Li, B., Li, S. & Sun, J. (2011). Isochron dating of sand-loess-soil deposits from the Mu Us Desert margin, central China. Quaternary Geochronology, 6 (6), 556-563.

Isochron dating of sand-loess-soil deposits from the Mu Us Desert margin, central China

Bo Li[1], Sheng-Hua Li[1*] Jimin Sun[2]

1. *Department of Earth Sciences, The University of Hong Kong, Pokfulam Road, Hong Kong, China*
2. *Institute of Geology and Geophysics, Chinese Academy of Sciences, P. O. Box 9825, Beijing 100029, China*

*Corresponding author. Email: shli@hku.hk

Abstract

A sand-loess-soil sequence from the margin of the Mu Us Desert was studied using the isochron infrared stimulated luminescence (IRSL) dating method utilizing K-feldspar grains extracted from sediments. Although the IRSL ages measured with the conventional method showed underestimation as a result of anomalous fading, the isochron results are broadly consistent with independent ages based on stratigraphic~~al~~ correlation in a glacial/interglacial scale over the last 250 ka. For samples older than 250 ka, the IRSL signals approached in field saturation and the isochron dating gave ambiguous results, suggesting an age limit for the method.

Keywords: Mu Us Desert, isochron dating, luminescence, Inner Mongolia, aeolian

1 Introduction

Sedimentary deposits in desert areas provide an important record of past climate change (Rognon, 1987; Lancaster, 1989; Petit-Maire and Page, 1992; Stokes et al., 1997; Thomas et al., 2000). In northern China, episodic dune formation and stabilization occurred during the Quaternary, associated with the waxing and waning of the East Asian monsoon (Sun et al., 1998; Sun et al., 1999). Particularly in the arid and semiarid regions, i.e. the transition zone between the desert and loess areas, the sediment record is highly sensitive to climate change and human impacts (Thompson et al., 1989; D'Arrigo et al., 2000; Sun, 2000; Li and Sun, 2006; Sun et al., 2006). As a result, the arid and semiarid areas in northern China form ideal regions for studying past climate changes and the relationship between climate change and human activities.

To reconstruct the palaeoclimate using information from sediments, one must have a chronological framework. In the past, dating of Holocene sediments in deserts and adjacent areas was mainly based on radiocarbon dating (Wang, 1992; Pachur et al., 1995; Li and Dong, 1998; Chen et al., 1999; An et al., 2000; Zhang et al., 2000; Zhou et al., 2001; Chen et al., 2003; Feng et al., 2006). However, the low organic carbon content and possible carbon contamination from the root of modern plants in arid areas limits the application of radiocarbon dating, or even invalidates it (Head et al., 1989; Birkeland, 1999). OSL dating of sediments from the desert areas in northern China has several advantages over radiocarbon dating. Firstly, the sediments in these areas are rich in quartz and feldspar, the minerals most suitable for OSL dating. Secondly, the mineral grains were transported a long distance by the strong wind, probably exposing them to sufficient daylight to zero the OSL signal; thus, the OSL 'clock' is likely to be well reset (Li et al., 2002). Finally, OSL dating has a greater age range and can be applied to sediments older than 50 ka, beyond the radiocarbon dating limit.

In the last a few years, OSL dating using quartz grains extracted from sediments has been successfully applied in reconstruction past environmental changes in arid and semi-arid regions in north China (Li et al., 2002; Li and Sun, 2006; Sun et al., 2006; Yang et al., 2006; Li et al., 2007b; Lu et al., 2007; Zhou et al., 2009). However, the quartz OSL signal saturates at relatively low doses and has made it difficult to use quartz for dating beyond (roughly) 70 thousand years (70 ka), unless the environmental dose rate is exceptionally low. In addition to that, underestimation in quartz OSL ages for old samples has been reported in the Chinese Loess Plateau (Buylaert et al., 2007; Lu et al., 2007; Qin and Zhou, 2009; Lai, 2010) and its northern margin area (Li and Li, 2006; Fan et al. 2011). Fan et al. (2011) found a ~50% underestimation in quartz OSL age using the single-aliquot regeneration (SAR) protocol for a ~55 ka sample extracted from a sedimentary layer containing stone tools from the bank of Salawusu River, Mu Us desert in central China. Hence, alternative dating techniques must

be explored in order to obtain a robust chronology framework for the aeolian deposits from the Mu Us Desert and the Chinese Loess Plateau.

An alternative mineral commonly used for OSL dating is feldspar. Optical dating of feldspar can undertaken using either visible wavelengths for stimulation or infrared (IR) stimulation; the latter gives rise to an infrared stimulated luminescence (IRSL) signal. The IRSL signal from potassium (K)-rich feldspars (KF) has several advantages over the OSL signal of quartz (Li et al. 2007b). Firstly, it has been found that the IRSL signal from sand-sized KF grains does not saturate until much higher doses are reached. Hence, it has great potential of extending the time frame for sedimentary deposits. In addition, the IRSL signal is bright compared with the quartz OSL signal, which enables high-precision luminescence measurements to be made. However, dating using the IRSL signal from sand-sized KF grains has not been adopted widely because of anomalous fading (Wintle, 1973; Spooner, 1992, 1994; Huntley and Lian, 2006), i.e. the IRSL signal decreases during storage at ambient temperature even though the relevant charges should be thermally stable over a much longer (geological) time period.

Recently, a new luminescence dating method, isochron IRSL dating, has been proposed (Li et al., 2008b); this uses the IRSL signal from KF grains of different grain sizes. This method has been found to avoid problems of anomalous fading of KF (Li et al., 2007a, 2008b) and the effects of past changes in environmental dose rate (Li et al., 2008a). This method has been tested using various samples from different regions of China and it has been found that it can provide reliable ages over the last 130 ka (Li et al., 2008b). In this paper, we apply the isochron dating technique to a sand/loess/palaeosol profile at the southeast margin of the Mu Us Desert, central China. We compare the isochron dating results with the ages based on stratigraphic~~al~~ correlation and test the old dating limitation of the isochron method.

2 Geological setting

The study site, the Shimao section, is located at the southeast margin of the Mu Us Desert (37°28'-39°23' N and 106°10'-110°30' E) (Fig. 1). This area lies within the East Asian monsoon zone with warm and humid air from the southeast in summer and cold and dry air from the north and west in winter (Chen, 1991); it is marked by semi-arid and sub-humid climate with a mean annual temperature ranging from 5.5 to 8.0°C and a mean annual precipitation ranging from 200 mm in the northwest to 450 mm in the southeast. More than 60% of the annual precipitation is received from July to September (Members of Loess Plateau Investigation Group, 1991). Stabilized and semi-stabilized sand dunes are widely distributed in the Mu Us Desert; ~64% of the area is occupied by

active dunes. Previous studies have suggested that the occurrence of the modern sand dunes is largely associated with the reworking of the ancient sands of the last glacial maximum (LGM) (Sun, 2000).

The Shimao section is a 76.7-m-thick aeolian sequence basically consisting of 40 alternated sand/loess/palaeosol layers (Fig. 2), which was deposited within about 580 ka (Sun et al., 1999). Each of the sand/loess/palaeosol layers is characterized by different grain sizes reflecting the energy of wind and different magnetic susceptibilities associated with the extent of pedogenesis, which reflects the waxing and waning of the East Asian Monsoon (Sun et al., 1999). A general description of the sequence has been given by Sun et al (1999). Previous chronology of the sequence was mainly based on correlation of the grain size curve to the orbitally tuned Baoji section (Ding et al., 1994) by assuming a continuous deposition. It has been shown that correlations of major stratigraphic units (in glacial/interglacial scale) between different sites in the Loess Plateau are reliable (Kukla and An, 1989; Ding et al., 1993). Hence, given the wide distribution of grain size and the well bleached nature, which is required for the isochron dating method, this profile provides an ideal example to test the age limit of isochron dating. In a recent study, 6 samples from the top 20m from this section has been dated using the isochron dating technique by Li et al. (2008b), and the results are found to be consistent with the those from stratigraph~~y~~ic correlation and quartz OSL ages. In the present study, we extend the application of isochron dating to the lower part of the section aiming to provide a cross-check for the limitation of isochron dating and the chronology of the section based on stratigraph~~y~~ic correlation.

3 Methods

A total of 10 OSL samples including the 6 samples reported by Li et al (2008) were collected from the section (Fig. 2). These include 9 samples from sand layers and one sample (Sm0404) from a loess layer (Fig. 2). Steel cylinders or aluminium cans 50 mm in diameter and 30 cm in length were pushed or hammered into a freshly-cleaned vertical section of the profile and immediately covered with a lid. In the laboratory, the two ends of the samples in the cylinders were first removed and collected for the estimation of the environmental dose rate. The remaining material was then treated with H_2O_2 and HCl to remove organic materials and carbonates. After that, various grain size fractions, 90-125, 125-150, 150-180, 180-212 and 212-250 μm, were separated for isochron dating. At least four grain size fractions were obtained from each sample. The KF grains were then separated by flotation in a heavy liquid with a density of 2.58 g/cm^3. The separated KF grains were treated with 10% HF for 40 minutes. All sample preparation procedures were performed under subdued red to orange light (>590 nm).

All IRSL measurements were performed using an automated Risø TL-DA-12 reader equipped with IR diodes. The IRSL signal from KF was detected through a Schott BG-39 filter combined with a Corning 7-59 filter. Irradiation was carried out using $^{90}Sr/^{90}Y$ beta sources attached to the reader. The dose rate has been calibrated for different grain sizes (Li et al. 2007a). For measurement, the separated mineral grains were mounted on 9.8-mm-diameter aluminium discs using Silkospray silicone oil.

The equivalent dose (D_e) of KF was determined using a SAR protocol (Murray and Wintle, 2000) with the use of a 10 s preheat at 280°C ahead of both the main IRSL measurement and the test dose measurement (Li et al., 2008b). The IRSL signal was measured at 60 °C for 300 s. The integral of the first 1 s of the OSL signal less the equivalent average signal in the last 5 s was used for calculation of D_e. Five regenerative doses, including a zero-dose and a recycling dose, were used for constructing growth curve. Aliquots with a recycling ratio falling out the range of 1.0±0.1 and zero-dose response (usually expressed as the ratio between the sensitivity corrected OSL signals for the zero dose and natural dose, and termed the recuperation ratio) higher than 5% were discarded for D_e determination (Murray and Wintle, 2000). For D_e determination, 6-8 aliquots were measured on average for each grain size. The relative standard error for each D_e estimate is generally less than 1%, confirming the high reproducibility of single-aliquot D_e measurements using IRSL from KF (e.g. Li et al., 2007b).

The environmental dose rates were measured using several techniques. The contribution from U and Th decay chains was determined using the thick-source alpha counting (TSAC) technique (Aitken, 1985). The K content was measured using X-ray fluorescence (XRF). Field water content was calculated from the sample weights before and after drying. The contribution from cosmic rays was calculated from the burial depth and the latitude and altitude of the samples (Prescott and Hutton, 1994).

4 Results

The D_e values, environmental dose rates and IRSL ages for 150-180μm KF from all samples are listed in Table 1 and the D_e values and IRSL ages plotted against sampling depth are shown in Fig. 2. Both the D_e values and IRSL ages increase with sampling depth for the upper 26 m of the sequence. The KF IRSL ages are within the range from 8.5±0.4 to 159±7 ka for the first 7 samples from Sm1 to Sm6. However, similar D_e values around 650 Gy and IRSL ages around 180 ka were obtained for the deepest (or oldest) samples Sm6', Sm7 and Sm8. A typical dose response curve of the IRSL signal from Sm8 was shown in Fig. 3. It demonstrates that the laboratory-regenerative signals grow up to a higher level than the natural signal and show no sign of saturation up to 1200 Gy. This suggests that the IRSL signal for these samples has reached 'field saturation', an equilibrium state between electron

capture in and escaping from the IRSL traps (Lamothe et al., 2003; Huntley and Lian, 2006; Li and Li, 2008).

The individual results from the isochron method using different grain sizes for all samples are shown in Figure 4. The D_e values increase with grain size, which is expected as larger grain sizes have higher internal dose rate. The internal dose rate for KF was calculated by assuming values of 13±1% and 400±100 ppm for potassium and rubidium, respectively. The choice of these values is based on the results and arguments of several previous studies (Huntley and Baril, 1997; Huntley and Hancock, 2001; Zhao and Li, 2005; Li et al., 2008b). Except for Sm8, a good linearity is observed between D_e values and the internal dose rates. This allows isochron ages to be estimated for all of our samples except Sm8, for which no dependence between D_e and internal dose rate was observed (Fig. 4).

The isochron ages against sampling depth are compared with the IRSL ages in Fig. 2. The ages obtained from the isochron method fall within the range of 10-250 ka. The IRSL ages and those derived from stratigraphic~~y~~ correlation (Fig. 13 in Sun et al., 1999) are compared in Fig. 5 (b). The IRSL ages show significant underestimation compared to the ages based on correlation, suggesting that the IRSL ages were underestimated. Such underestimation can be explained in terms of anomalous fading, as a result of which IRSL signals from feldspar decrease with storage time at room temperature (Wintle, 1973; Spooner, 1992, 1994; Huntley and Lamothe, 2001; Huntley and Lian, 2006). Li and Li (2008) reported a fading rate of ~3%/decade after laboratory irradiation for KF from the Shimao section. It is thus concluded that the IRSL ages from the Shimao section are underestimated as a result of anomalous fading.

5 Discussion

5.1 The isochron chronology of the Shimao section in the last 250 ka

The aeolian sand, palaeosols and loess layers from the desert-loess boundary have been suggested as indicatives of the retreat and advance of the Mu Us Desert, which is thought to have been driven by the variation in the extent of aeolian activity, vegetation cover, and precipitation (Dong et al., 1989; Sun and Ding, 1998; Sun et al., 1999). The sand layers presumably reflect the south-eastward extensions of the Mu Us Desert in response to the enhanced winter monsoon. The palaeosol layers would then have developed during warm and humid episodes, indicating the retreat of the desert under a condition of reduced aeolian activity, greater vegetation cover and much enhanced prevailing summer monsoon. The loess layers accumulated under an intermediate climatic

condition between the two extreme climates for sand accumulation and soil development. Dating of these layers provides thus an estimation of the history of desert retreat and advance.

The isochron ages for samples Sm1, Sm2, Sm3, Sm4, Sm0404, Sm5 and Sm6 and magnetic susceptibility variations plotted against depth for the upper 30 m of the section are compared with the marine oxygen isotopic record (SPECMAP) (Imbrie et al., 1984) in Fig. 5. The ages for these samples are generally in stratigraphic~~al~~ order and increase with sample depth (Fig. 2). The isochron dating results are broadly consistent with the previous chronology framework based on stratigraphic~~al~~ correlation (Sun et al., 1999) (Fig. 5(a)). This provides a cross-check on the validity of the two independent dating methods. The age of sample Sm1 and Sm2 are 10.9±1.5 and 8.5±1.2 ka, respectively. It is noted that the isochron ages of both samples are consistent with quartz OSL ages (Li et al., 2008b) but lower than the correlation ages, i.e. 20±1 and 25±1 ka. Since OSL dating only record the time since the last exposure to sunlight, the discrepancy between OSL ages and correlation ages suggests that the sand layer was developed during the last glacial maximum (LGM) (or oxygen isotopic stage 2) but was not finally stabilize until the early Holocene. During the LGM period, widespread aeolian sand mobilization still occurred in this region, which caused the materials of sand dunes exposed to sunlight repeatedly, resetting the OSL 'clock' to zero until the early Holocene when and they were stabilized. This age also confirms that the uppermost palaeosol, denoted S0, developed after the early Holocene.

Samples Sm3 and Sm4 gave isochron ages of 40.8±6.4 and 40.3±5.6 ka, respectively. These ages are indistinguishable, and fall within the age range of OIS 3, i.e. from 59 to 29 ka (Voelker, 2002; Thompson and Goldstein, 2006), indicating that the two sand layers from which the samples Sm3 and Sm4 were taken and the loess layer between them were deposited during stadials and interstadials in the last glacial cycle. This also confirms that the L1 unit, consisting of three sand layers and two loess layers, was deposited during the last glacial period. It is noted that the sample Sm4 from the sand layer immediately above 'S1' was previously thought to have been deposited during OIS 4 (Sun et al., 1999), with a correlation age of ~70 ka. However, the isochron dating result for sample Sm4 (40.3±5.6 ka) suggests that this layer is actually corresponding to OIS 3. This may indicate that the materials formed during OIS 4 had undergone repeated reworking and mobilization due to the high mobility of the aeolian sediments in the cold/dry condition during OIS 4 in this region. These sand deposits were finally stabilized in a warmer/wetter condition during OIS 3.

Sample Sm0404, taken from the second loess layer within 'S1', gave an isochron age of 92±20 ka, consistent with OIS 5 (Fig. 6). This suggests that the 'S1' layer, including three palaeosol layers and two interbedded loess layers, formed during the last interglacial (OIS 5). This is further supported by the age of 121±26 ka for the sample Sm5 taken from the underlying sand layer. The age of Sm5

also indicates that L2 was developed during glacial period corresponding to OIS 6. The S2 unit consists of two thick palaeosol beds and an interbedded sand bed, and it appears to have formed during the interglacial period associated with OIS 7 (Fig. 6), as inferred by the age of 223±33 ka for sample Sm6 (from the interbedded sand bed). Our dating results support the suggestion that the sand deposits mainly occur during glacial periods, while soil could only develop during interglacial periods (Fig. 6).

5.2 The limit of isochron dating

By dating a series of samples from the Shimao section from the top of L1 to the bottom of L5 using the isochron dating technique, the age was found to increase with sampling depth for the samples from Sm1 to Sm6 (Fig. 4 and Fig. 6). The oldest isochron age obtained, i.e. 223±33 ka, is for the sample Sm6 taken from the palaeosol bed S2. It is interesting to note that the isochron age started to decrease with depth (or deposition age) for samples Sm6', Sm7 and Sm8 (Fig. 4), although they should be older than the samples above. The isochron dating results for samples Sm6' and Sm7 are 168±35 ka and 82±9 ka, respectively (Fig. 4). No isochron ages were obtained for Sm8 because no dependence of D_e against the internal dose rate was observed (Fig. 4). The apparent IRSL ages of the samples from the upper part of the section increase monotonically from 8.5 ka for Sm1 to 156 ka of Sm6, as expected from their depth (Fig. 2). However, the apparent IRSL ages for samples Sm6' (180±7 ka), Sm7 (178±11 ka) and Sm8 (194±8 ka) from the lower part of the section are similar to each other within the errors, although their geological ages presumably differ significantly, based on their stratigraphical locations. It is thus concluded that the IRSL signals for sample Sm6', Sm7 and Sm8 have reached 'field saturation' or 'field equilibrium' i.e. the condition where the rate of electron filling of IRSL traps equals the rate of escaping, such that the net trap population becomes constant (Lamothe et al., 2003; Huntley and Lian, 2006; Li and Li, 2008).

For the field-saturated samples, e.g. Sm8, all grains saturate at about 650 Gy, independent of size (Fig. 4). This maximum dose that can be recorded by the IRSL signal is much lower than the expected saturation dose derived from the laboratory growth curve (Fig. 3), which shows no saturation up to ~1200 Gy. A reasonable explanation for this observation is that anomalous fading occurred for both the internal dose and external dose for these samples, which is contradict to the observation that the isochron ages for the younger samples agree with the age control (Li et al. 2008) although underestimation in ages would be derived from a conventional IRSL SAR method. Whatever the reason for these contradictions, they suggest an increasing inaccuracy or underestimation in isochron ages for older samples close to saturation. It is thus suggested that the isochron method can only be applied to those samples with natural doses below ~86% of the natural saturation dose,

according to the $2D_0$ argument (Wintle and Murray, 2006), i.e. when the conventional IRSL doses from the largest grains are within ~86% of 'field saturation' (~500-550 Gy for the samples in this study) then one should be suspicious of the isochron ages. This provides a rough estimation for the limit of reliable isochron ages, of ~200-250 ka.

6 Conclusions

Sand-loess-soil sequences of the Shimao section from the margin of the Mu Us Desert were dated using the isochron IRSL method using K-feldspar grains extracted from sediments. The isochron results provide an absolute chronological framework for the sequence back to ~250 ka. Although the IRSL ages underestimate the expected ages (20% in average), the isochron ages were broadly consistent with the expected ages back to 250 ka based on stratigraphic~~al~~ correlation with a glacial/interglacial scale. Our dating results indicate that the sedimentary features in this area are sensitive to past climate changes. The sand layers mainly developed during glacial periods, and presumably reflect the south-eastward extensions of the Mu Us Desert in response to the enhanced winter monsoon. The palaeosol layers, formed during interglacial periods, reflect the retreat of the desert during periods of reduced aeolian activity, greater vegetation cover and enhanced prevailing summer monsoon.

Acknowledgements

We thank Andrew Murray, David Huntley and an anonymous reviewer for comments. The study is financially supported by grants to SHL from the Research Grant Council of the HKSAR, China (Project No. 7035/06P, 7035/07P and 7028/08P).

References

Adamiec, G., Aitken, M. J. (1998), Dose-rate conversion factors: Update, *Ancient TL* **16**, 37– 50.

Aitken, M.J., 1985. *Thermoluminescence dating*. Academic press London.

An, Z.S., Porter, S.C., Kutzbach, J.E., Wu, X.H., Wang, S.M., Liu, X.D., Li, X.Q., Zhou, W.J., 2000. Asynchronous Holocene optimum of the East Asian monsoon. *Quaternary Science Reviews* **19**, 743-762.

Buylaert, J.P., Vandenberghe, D., Murray, A.S., Huot, S., De Corte, F., Van den Haute, P., 2007. Luminescence dating of old (>70ka) Chinese loess: A comparsion of single-aliquot OSL and IRSL techniques. *Quaternary Geochronology* **2**, 9-14.

Chen, C.T.A., Lan, H.C., Lou, J.Y., Chen, Y.C., 2003. The dry Holocene Megathermal in Inner Mongolia. *Palaeogeography Palaeoclimatology Palaeoecology* **193**, 181-200.

Chen, F.H., Shi, Q., Wang, J.M., 1999. Environmental changes documented by sedimentation of Lake Yiema in arid China since the Late Glaciation. *Journal of Paleolimnology* **22**, 159-169.

Chen, L.X., 1991. *East Asian Monsoon*. Meteorology Press Beijing.

D'Arrigo, R., Jacoby, G., Pederson, N., Frank, D., Buckley, B., Nachin, B., Mijiddorj, R., Dugarjav, C., 2000. Monogolian tree-rings, temperature sensitivity and reconstructions of Northern Hemisphere temperature. *Holocene* **10**, 669-672.

Ding, Z. L., Rutter, N. W., and Liu, T. S., Pedostratigraphy of Chinese loess deposits and climatic cycles in the last 2.5Myr, Catena, 20(1993), 73-91.

Ding, Z., Yu, Z., Rutter, N.W., Liu, T., 1994. Towards an orbital time-scale for Chinese loess deposits. *Quaternary Science Reviews* **13**, 39-70.

Dong, G.R., Gao, S.Y., Jin, J., Li, B.S., 1989. The Formation, Evolution and Cause of the Mu-Us Desert in China. *Science in China Series B-Chemistry* **32**, 859-872.

Fain, J., Soumana, S., Montret, M., Miallier, D., Pilleyre, T., Sanzelle, S., 1999. Luminescence and ESR dating - Beta-dose attenuation for various grain shapes calculated by a Monte-Carlo method. *Quaternary Science Reviews* **18**, 231-234.

Fan, A.C., Li, S.H., Li, B., 2011. Observation of unstable fast component in OSL of quartz. *Radiation Measurements* **46**, 21-28.

Feng, Z.D., An, C.B., Wang, H.B., 2006. Holocene climatic and environmental changes in the arid and semi-arid areas of China: a review. *Holocene* **16**, 119-130.

Members of Loess Plateau Investigation Group, 1991. *Land Desertification in the Northern Loess Plateau*. Science Press Beijing (in Chinese).

Head, M.J., Zhou, W.J., Zhou, M.F., 1989. Evaluation of C-14 Ages of Organic Fractions of Paleosols from Loess-Paleosol Sequences near Xian, China. *Radiocarbon* **31**, 680-696.

Huntley, D.J., Baril, M.R., 1997. The K content of the K-feldspars being measured in optical dating or in thermoluminescence dating. *Ancient TL* **15**, 11-13.

Huntley, D.J., Hancock, R.G.V., 2001. The Rb contents of the K-feldspars being measured in optical dating. *Ancient TL* **19**, 43-46.

Huntley, D. J., Lamothe, M., 2001. Ubiquity of anomalous fading in K-feldspars and the measurement and correction for it in optical dating. *Can. J. Earth Sci.* **38**, 1093– 1106, doi:10.1139/cjes-38-7-1093.

Huntley, D.J., Lian, O.B., 2006. Some observations on tunnelling of trapped electrons in feldspars and their implications for optical dating. *Quaternary Science Reviews* **25**, 2503-2512.

Imbrie, J., Haye, J.D., Martinson, D.B., McIntyre, A., Mix, A.C., Morley, J.J., Pisias, N.G., Prell, W.L., Shackleton, N.J. (Eds.), 1984. The orbital theory of Pleistocene climate: support from a revised chronology of the marine $\delta^{18}O$ record. Reidel, Dordrecht.

Kukla, G., An, Z., 1989. Loess stratigraphy in Central China. *Palaeogeography, Palaeoclimatology and Palaeoecology* 72, 203–225.

Lai, Z.P., 2010. Chronology and the upper dating limit for loess samples from Luochuan section in the Chinese Loess Plateau using quartz OSL SAR protocol. *Journal of Asian Earth Sciences* **37**, 176-185.

Lamothe, M., Auclair, M., Hamzaoui, C., Huot, S., 2003. Towards a prediction of long-term anomalous fading of feldspar IRSL. *Radiation Measurements* **37**, 493-498.

Lancaster, N., 1989. Late Quaternary Paleoenvironments in the Southwestern Kalahari. *Palaeogeography Palaeoclimatology Palaeoecology* **70**, 367-376.

Li, B., Li, S. H., 2006. Comparison of D-e estimates using the fast component and the medium component of quartz OSL. *Radiation Measurements* **41**, 125-136.

Li, B., Li, S.H., 2008. Investigations of the dose-dependent anomalous fading rate of feldspar from sediments. *Journal of Physics D-Applied Physics* **41**, 225502.

Li, B., Li, S.H., Wintle, A.G., 2008a. Overcoming environmental dose rate changes in luminescence dating of waterlain deposits. *Geochronometria* **30**, 33-40.

Li, B., Li, S.H., Wintle, A.G., Zhao, H., 2007a. Isochron measurements of naturally irradiated K-feldspar grains. *Radiation Measurements* **42**, 1315-1327.

Li, B., Li, S.H., Wintle, A.G., Zhao, H., 2008b. Isochron dating of sediments using luminescence of K-feldspar grains. *Journal of Geophysical Research-Earth Surface* **113**, F02026, doi:02010.01029/02007JF000900. .

Li, S.H., Chen, Y.Y., Li, B., Sun, J.M., Yang, L.R., 2007b. OSL dating of sediments from desert in northern China. *Quaternary Geochronology* **2**, 23-28.

Li, S.H., Sun, J.M., 2006. Optical dating of Holocene dune sands from the Hulun Buir Desert, northeastern China. *Holocene* **16**, 457-462.

Li, S.H., Sun, J.M., Zhao, H., 2002. Optical dating of dune sands in the northeastern deserts of China. *Palaeogeography Palaeoclimatology Palaeoecology* **181**, 419-429.

Li, X.Z., Dong, G.R., 1998. Preliminary studies on formative age and causes of Hunshandake Sandy Land in China (in Chinese). *Journal of Desert Research* **18**, 16-20.

Lu, Y.C., Wang, X.L., Wintle, A.G., 2007. A new OSL chronology for dust accumulation in the last 130,000 yr for the Chinese Loess Plateau. *Quaternary Research* **67**, 152-160.

Murray, A.S., Wintle, A.G., 2000. Luminescence dating of quartz using an improved single-aliquot regenerative-dose protocol. *Radiation Measurements* **32**, 57-73.

Pachur, H.J., Wunnemann, B., Zhang, H., 1995. Lake Evolution in the Tengger Desert, Northwestern China, during the Last 40,000 Years. *Quaternary Research* **44**, 171-180.

Petit-Maire, N., Page, N., 1992. Remote-Sensing and Past Climatic Changes in Tropical Deserts - Example of the Sahara. *Episodes* **15**, 113-117.

Prescott, J.R., Hutton, J.T., 1994. Cosmic-Ray Contributions to Dose-Rates for Luminescence and Esr Dating - Large Depths and Long-Term Time Variations. *Radiation Measurements* **23**, 497-500.

Qin, J.T., Zhou, L.P., 2009. Stepped-irradiation SAR: A viable approach to circumvent OSL equivalent dose underestimation in last glacial loess of northwestern China. *Radiation Measurements* **44**, 417-422.

Readhead, M.L., 2002. Absorbed dose fraction for ^{87}Rb β particles. *Ancient TL* **20**, 25-27.

Rognon, P., 1987. Late Quaternary Climatic Reconstruction for the Maghreb (North-Africa). *Palaeogeography Palaeoclimatology Palaeoecology* **58**, 11-34.

Spooner, N.A., 1992. Optical dating: preliminary results on the anomalous fading of luminescence from feldspars. *Quaternary Science Reviews* **11**, 139-145.

Spooner, N.A., 1994. The anomalous fading of infrared-stimulated luminescence from feldspars. *Radiation Measurements* **23**, 625-632.

Stokes, S., Thomas, D.S.G., Washington, R., 1997. Multiple episodes of aridity in southern Africa since the last interglacial period. *Nature* **388**, 154-158.

Sun, J.M., 2000. Origin of eolian sand mobilization during the past 2300 years in the Mu Us Desert, China. *Quaternary Research* **53**, 78-88.

Sun, J.M., Ding, Z.L., 1998. Deposits and soils of the past 130,000 years at the desert-loess transition in northern China. *Quaternary Research* **50**, 148-156.

Sun, J.M., Ding, Z.L., Liu, T.S., Rokosh, D., Rutter, N., 1999. 580,000-year environmental reconstruction from aeolian deposits at the Mu Us Desert margin, China. *Quaternary Science Reviews* **18**, 1351-1364.

Sun, J.M., Li, S.H., Han, P., Chen, Y.Y., 2006. Holocene environmental changes in the central Inner Mongolia, based on single-aliquot-quartz optical dating and multi-proxy study of dune sands. *Palaeogeography Palaeoclimatology Palaeoecology* **233**, 51-62.

Thomas, D.S.G., O'Connor, P.W., Bateman, M.D., Shaw, P.A., Stokes, S., Nash, D.J., 2000. Dune activity as a record of late Quaternary aridity in the Northern Kalahari: new evidence from northern Namibia interpreted in the context of regional arid and humid chronologies. *Palaeogeography Palaeoclimatology Palaeoecology* **156**, 243-259.

Thompson, L.G., Mosleythompson, E., Davis, M.E., Bolzan, J.F., Dai, J., Yao, T., Gundestrup, N., Wu, X., Klein, L., Xie, Z., 1989. Holocene Late Pleistocene Climatic Ice Core Records from Qinghai-Tibetan Plateau. *Science* **246**, 474-477.

Thompson, W.G., Goldstein, S.L., 2006. A radiometric calibration of the SPECMAP timescale. *Quaternary Science Reviews* **25**, 3207-3215.

Voelker, A.H.L., 2002. Global distribution of centennial-scale records for Marine Isotope Stage (MIS) 3: a database. *Quaternary Science Reviews* **21**, 1185-1212.

Wang, W.F., 1992. Preliminary study on the environmental changes of Hulun Buir Sandy Land since the Holocene (in Chinese). *Journal of Desert Research* **12**, 13-19.

Wintle, A.G., 1973. Anomalous fading of thermoluminescence in mineral samples. *Nature* **245**, 143-144.

Wintle, A.G., Murray, A.S., 2006. A review of quartz optically stimulated luminescence characteristics and their relevance in single-aliquot regeneration dating protocols. *Radiation Measurements* **41**, 369.

Yang, X.P., Preusser, F., Radtke, U., 2006. Late Quaternary environmental changes in the Taklamakan Desert, western China, inferred from OSL-dated lacustrine and aeolian deposits. *Quaternary Science Reviews* **25**, 923-932.

Zhang, H.C., Ma, Y.Z., Wunnemann, B., Pachur, H.J., 2000. A Holocene climatic record from arid northwestern China. *Palaeogeography Palaeoclimatology Palaeoecology* **162**, 389-401.

Zhao, H., Li, S.H., 2005. Internal dose rate to K-feldspar grains from radioactive elements other than potassium. *Radiation Measurements* **40**, 84-93.

Zhou, W.J., Head, M.J., Deng, L., 2001. Climate changes in northern China since the late Pleistocene and its response to global change. *Quaternary International* **83/85**, 285-292.

Zhou, Y.L., Lu, H.Y., Zhang, J.F., Mason, J.A., Zhou, L.P., 2009. Luminescence dating of sand-loess sequences and response of Mu Us and Otindag sand fields (north China) to climatic changes. *Journal of Quaternary Science* **24**, 336-344.

Figure captions:

Figure 1: Map showing the Mu Us desert and the Shimao section.

Figure 2: Stratigraphy, sampling positions, K-feldspar IRSL D_e, IRSL ages and isochron ages of the Shimao section. The stratigraphy is from Sun et al. (1999).

Figure 3: Dose response curve of K-feldspar from sample Sm8.

Figure 4: Isochron plots of all samples. The D_e values are shown as a function of the internal beta dose rate (x-axis), calculated by assuming that the concentrations of K and Rb are 13% and 400 μg/g (Huntley and Baril, 1997; Huntley and Hancock, 2001; Zhao and Li, 2005), respectively, and using the absorbed beta dose fraction for the ^{40}K and the ^{87}Rb emissions (Fain et al., 1999; Readhead, 2002). The full line is the best fitted line of the data points. The dashed line is calculated using the method described by Li et al. (2008b) and the age calculated from the difference between the slopes of the two lines (see Li et al. (2008b) for a full description of the method).

Figure 5: (a) Comparison between the isochron IRSL ages and those based on stratigraphic~~al~~ correlation (Fig. 13 in Sun et al., 1999). (b) Comparison between the KF IRSL ages obtained for 150-180μm grains and those based on stratigraphic~~al~~ correlation.

Figure 6: Stratigraphy, isochron ages, magnetic susceptibility (MS) curve and the SPECMAP oxygen isotope curve for the last 300 ka. The oxygen isotopic stages are shown in numbers. Note the different units of the y-axis of the MS curve (depth) and the SPECMAP curve (age).

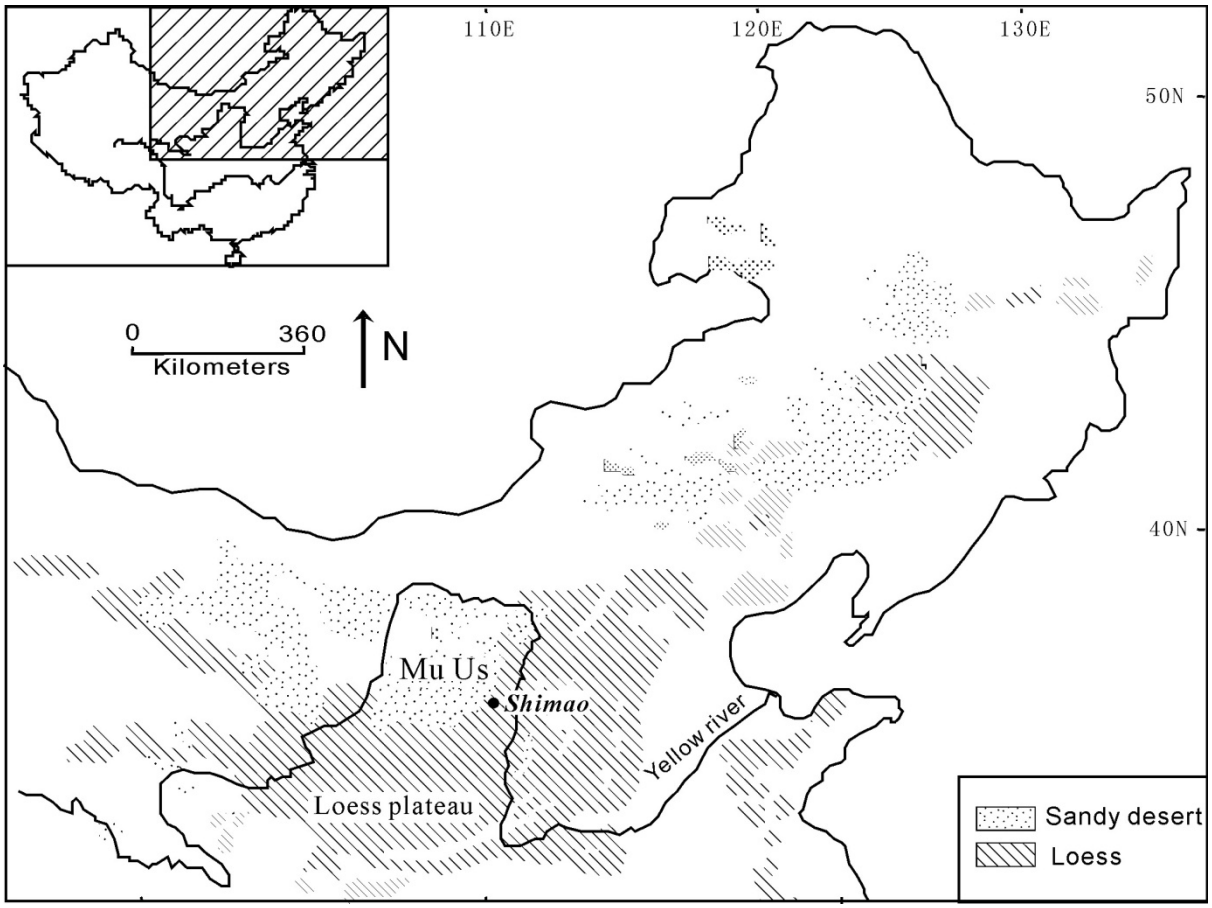
110E
120E
130E
50N
40N
0
360
Kilometers
N
Mu Us
Shimao
Yellow river
Loess plateau
Sandy desert
Loess

Figure 1

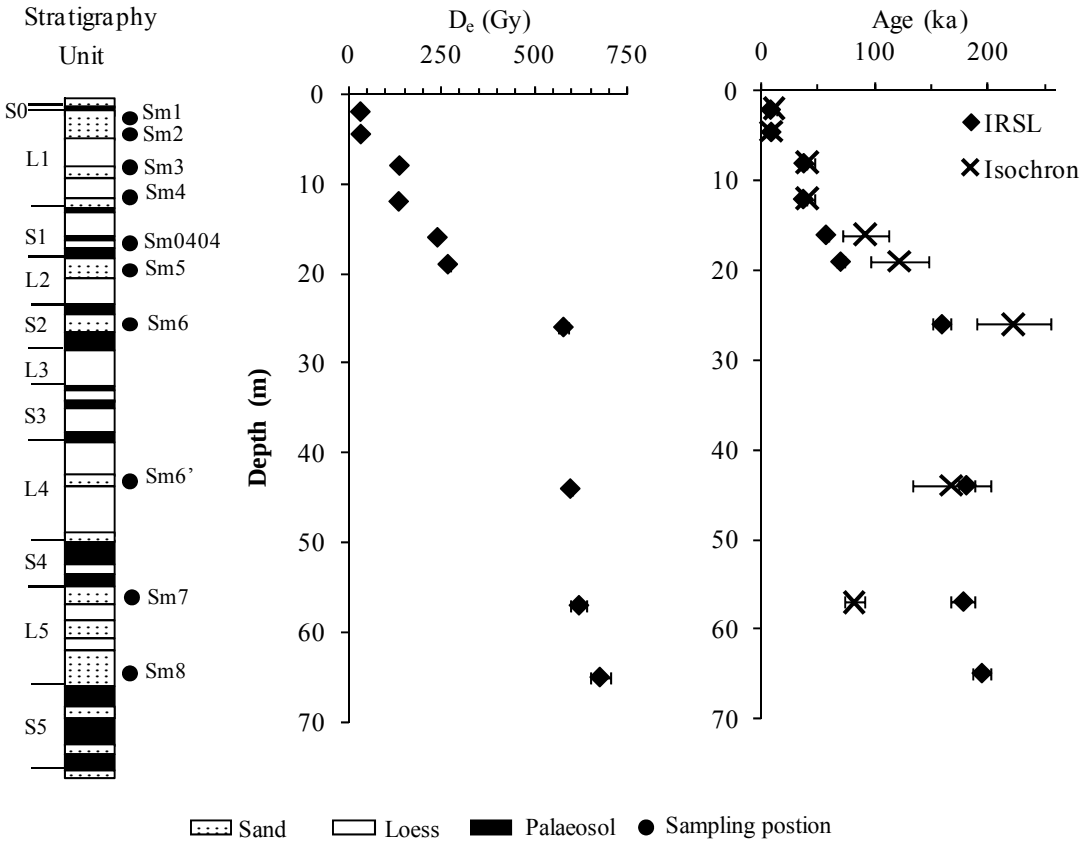
Stratigraphy
Unit
S0
L1
S1
L2
S2
L3
S3
L4
S4
L5
S5
Sm1
Sm2
Sm3
Sm4
Sm0404
Sm5
Sm6
Sm6'
Sm7
Sm8
De (Gy)
0
250
500
750
Depth (m)
0
10
20
30
40
50
60
70
Age (ka)
0
100
200
IRSL
Isochron
Sand
Loess
Palaeosol
Sampling postion

Figure 2

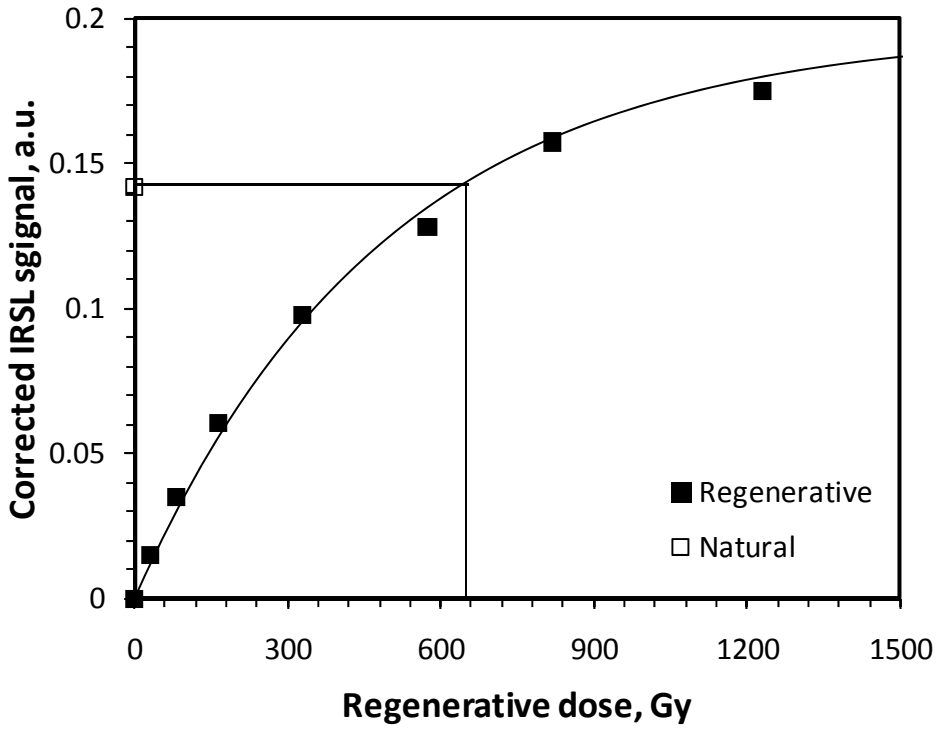
0.2
0.15
0.1
0.05
0
Corrected IRSL sgignal, a.u.
0
300
600
900
1200
1500
Regenerative dose, Gy
Regenerative
Natural

Figure 3

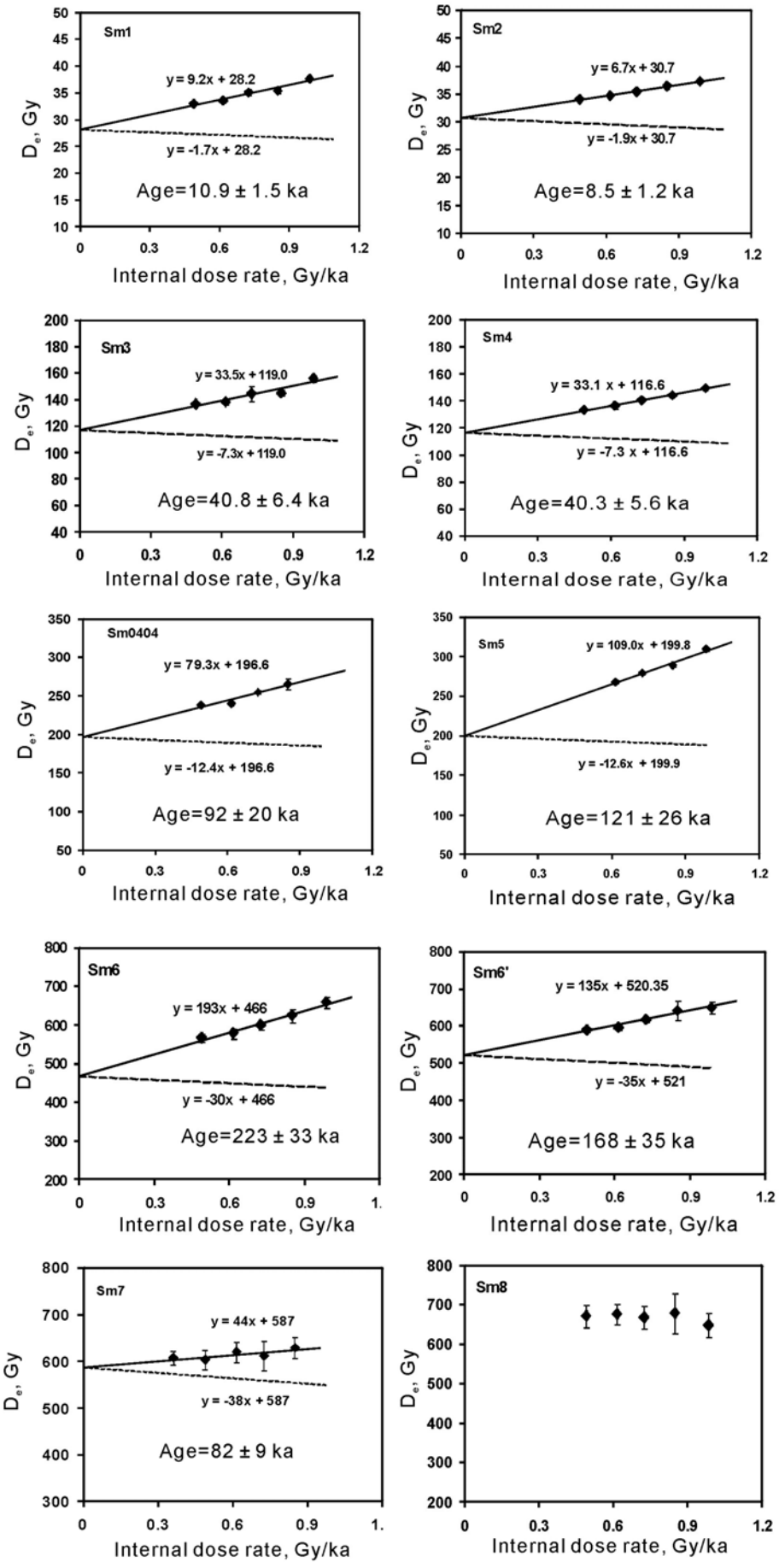
Sm1
y = 9.2x + 28.2
y = -1.7x + 28.2
Age=10.9 ± 1.5 ka
Sm2
y = 6.7x + 30.7
y = -1.9x + 30.7
Age=8.5 ± 1.2 ka
Sm3
y = 33.5x + 119.0
y = -7.3x + 119.0
Age=40.8 ± 6.4 ka
Sm4
y = 33.1 x + 116.6
y = -7.3 x + 116.6
Age=40.3 ± 5.6 ka
Sm0404
y = 79.3x + 196.6
y = -12.4x + 196.6
Age=92 ± 20 ka
Sm5
y = 109.0x + 199.8
y = -12.6x + 199.9
Age=121 ± 26 ka
Sm6
y = 193x + 466
y = -30x + 466
Age=223 ± 33 ka
Sm6'
y = 135x + 520.35
y = -35x + 521
Age=168 ± 35 ka
Sm7
y = 44x + 587
y = -38x + 587
Age=82 ± 9 ka
Sm8
De, Gy
Internal dose rate, Gy/ka

Figure 4

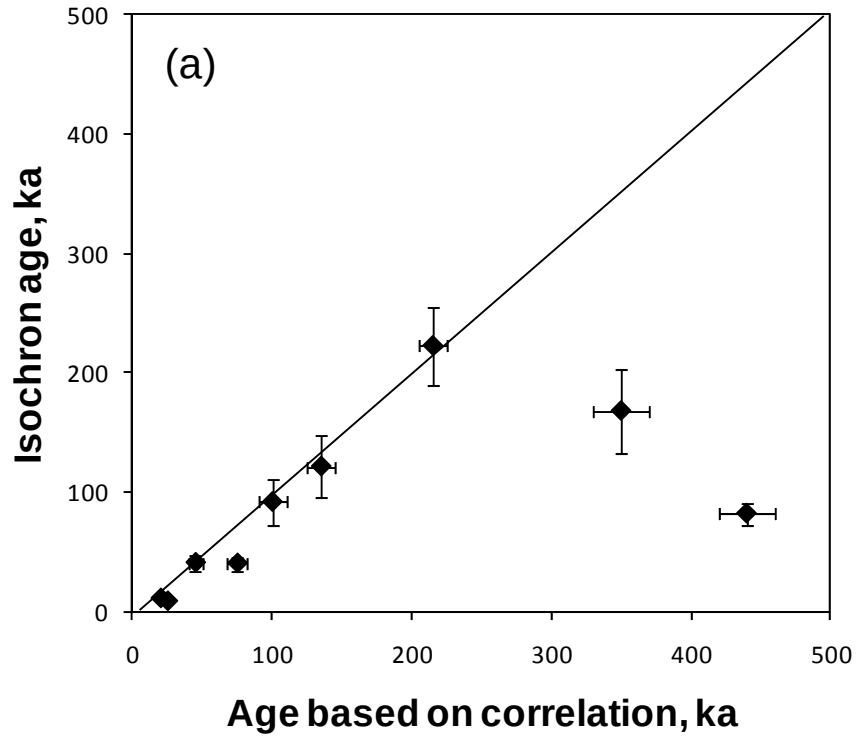
(a)
Isochron age, ka
Age based on correlation, ka
0
100
200
300
400
500

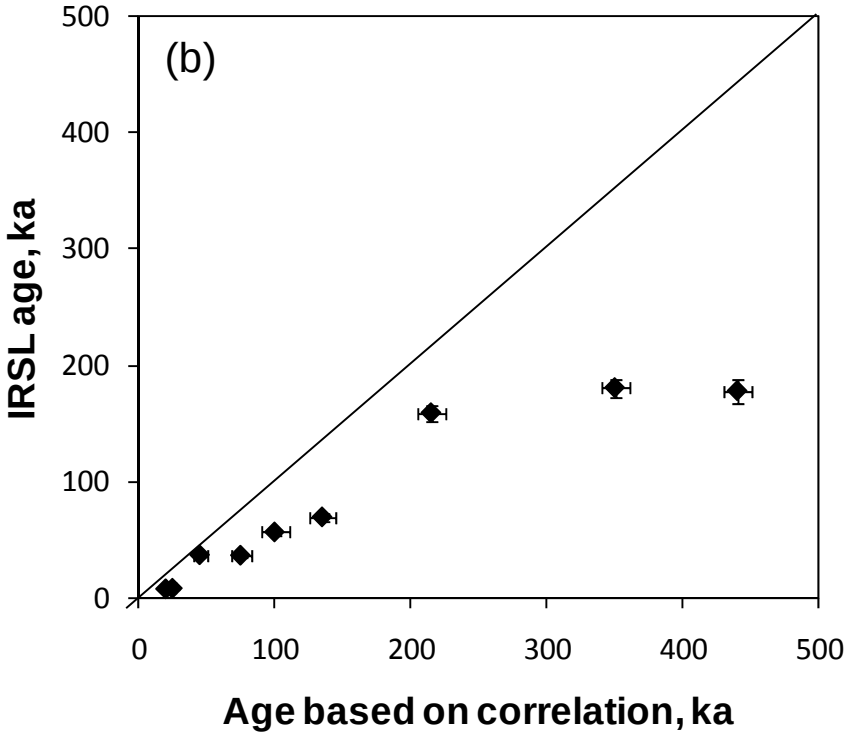
(b)
IRSL age, ka
Age based on correlation, ka
0
100
200
300
400
500

Figure 5

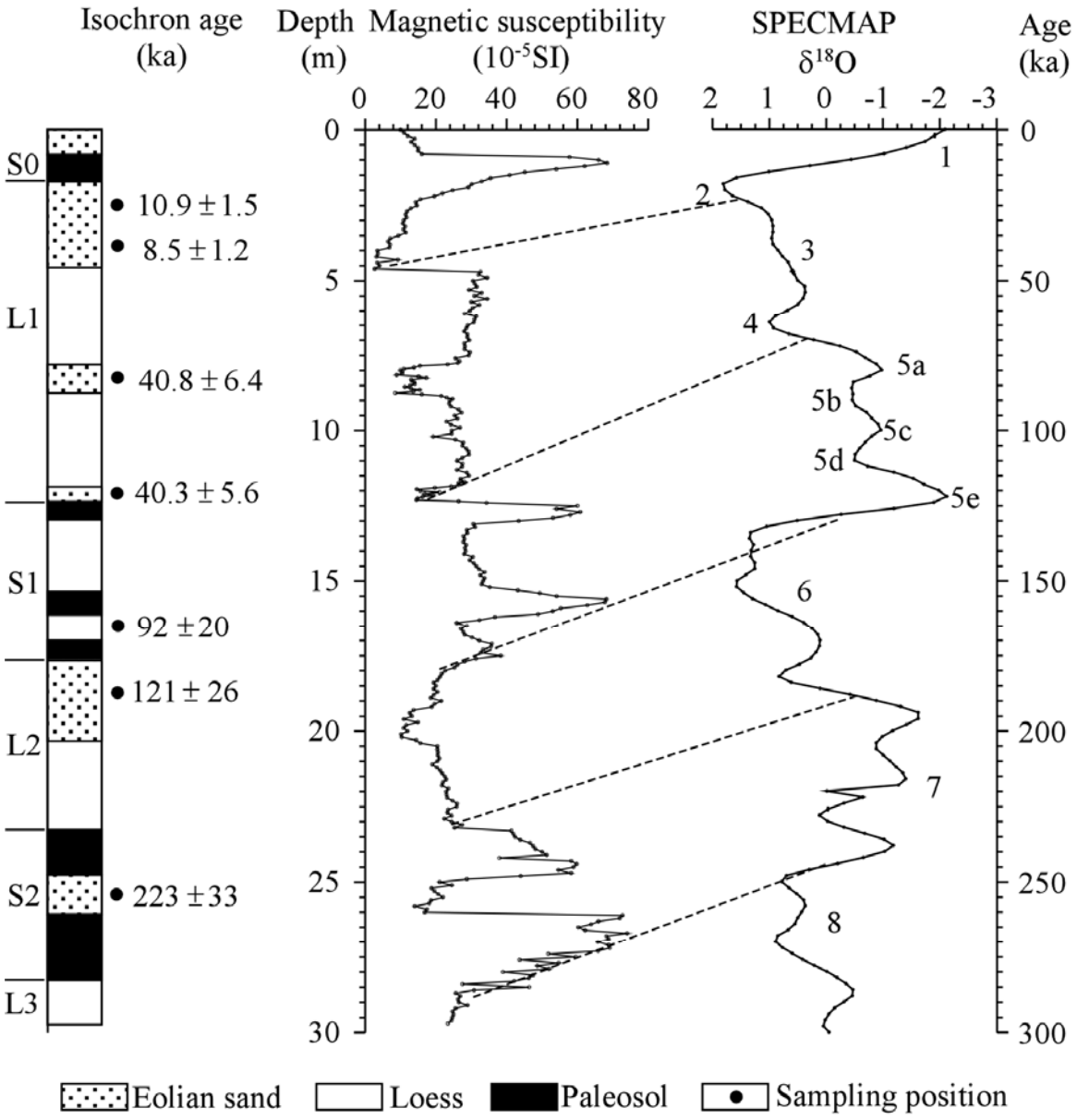
Isochron age (ka)
Depth (m)
Magnetic susceptibility (10^{-5}SI)
SPECMAP $\delta^{18}O$
Age (ka)
S0
L1
S1
L2
S2
L3
10.9 ± 1.5
8.5 ± 1.2
40.8 ± 6.4
40.3 ± 5.6
92 ± 20
121 ± 26
223 ± 33
1
2
3
4
5a
5b
5c
5d
5e
6
7
8
Eolian sand
Loess
Paleosol
Sampling position

Figure 6

Table 1: Equivalent dose, dose rate, KF IRSL ages, isochron dating results and stratigraphic~~al~~ correlation ages.

Sample	Depth (cm)	Alpha counting rate [a] (cts/1000s)	K content (%)	Water content (%)	Cosmic ray (Gy/ka)	Equivalent dose (Gy)	Ext. Dose rate [b] (Gy/ka)	Int. Dose rate [b,c] (Gy/ka)	IRSL age (ka)	Isochron age (ka)	Correlation age d
Sm1	2	5.10±0.13	2.5	4±2	0.16	33.5±0.4	3.3±0.2	0.62±0.05	8.5±0.4	10.9±1.5	20±1
Sm2	4.5	4.86±0.12	2.5	4±2	0.12	34.7±0.4	3.2±0.2	0.62±0.05	9.0±0.5	8.5±1.2	25±1
Sm3	8	4.97±0.13	2.3	4±2	0.08	138±2	3.1±0.2	0.62±0.05	38±2	41±6.4	45±5
Sm4	12	5.05±0.13	2.3	4±2	0.05	136±2	3.0±0.2	0.62±0.05	37±2	40±5.6	70±5
Sm0404	16	12.27±0.24	2.2	5±2	0.04	240±3	3.6±0.2	0.62±0.05	57±2	92±20	100±10
Sm5	19	7.06±0.17	2.2	4±2	0.03	268±4	3.2±0.2	0.62±0.05	70±3	121±26	135±10
Sm6	26	5.59±0.15	2.2	4±2	0.02	578±14	3.0±0.1	0.62±0.05	159±7	223±33	215±10
Sm6'	44	2.50±0.10	2.5	4±2	0.02	597±6	2.7±0.1	0.62±0.05	180±7	168±35	350±20
Sm7	57	4.60±0.14	2.4	4±2	0.01	620±21	2.9±0.1	0.62±0.05	178±11	82±9	440±20
Sm8	65	3.47±0.13	2.4	4±2	0	676±26	2.8±0.1	0.62±0.05	194±8	-	470±20

[a] The α-count rate is measured using 42-mm-diameter ZnS screens.

[b] The internal dose rate and external dose rate are calculated for an average grain size of 150-180 μm using the dose rate conversion factors of Adamiec and Aitken (1998) and absorbed dose fraction for ^{87}Rb of Readhead, (2002).

[c] The internal dose rate for KF was calculated by assuming values of 13±1% and 400±100 ppm for potassium and rubidium, respectively (Huntley and Baril, 1997; Huntley and Hancock, 2001; Zhao and Li, 2005; Li et al., 2008b).

[d] The correlation ages were estimated from the figure 13 from Sun et al (1999), together with the sampling positions.